Supplementary Information (SI) for Journal of Materials Chemistry A.
This journal is © The Royal Society of Chemistry 2026

# Supplementary Information -

# Ge-Induced Cation Ordering for Enhanced Thermoelectric Performance in $AgSbTe_2$

Kivanc Saglik [a,b], Jinfeng Dong [a], Dongwang Yang [a,c], Erhai Hu [a], Han Yan [a], Zheng Liu [a], Qiang Zhu [b,d], Ady Suwardi [e], Xizu Wang [b,*], Qingyu Yan [a,*]

[a] School of Materials Science and Engineering, Nanyang Technological University, 50 Nanyang Ave, Block N4.1, Singapore 639798, Republic of Singapore

[b] Institute of Materials Research and Engineering (IMRE), Agency for Science, Technology, and Research (A*STAR), 2 Fusionopolis Way, Singapore 138634, Republic of Singapore.

[c] State Key Laboratory of Advanced Technology for Materials Synthesis and Processing, Wuhan University of Technology, Wuhan, 430070, China

[d] Institute of Sustainability for Chemicals, Energy and Environment ($ISCE^2$), Agency for Science, Technology, and Research ($A^*STAR$), 1 Pesek Road, Jurong Island, 627833, Singapore

[e] Department of Electrical Engineering, The Chinese University of Hong Kong (CUHK), Central Ave, Hong Kong, 999077

[*] Email: alexyan@ntu.edu.sg & wangxz@a-star.edu.sg

**Lattice Parameters Calculations**

The lattice parameters of $AgSbTe_2$ were determined from the powder XRD data using the relations below:

**Equation 1**: Bragg's law: $d = \lambda/2\sin\theta$

In this relation, $d$ denotes the interplanar spacing, $\lambda$ is the X-ray wavelength (1.54 Å for Cu Kα radiation), and $2\theta$ is the corresponding diffraction angle.

**Equation 2**: $a = b = c = d\sqrt{h^2 + k^2 + l^2}$

In this expression, a = b = c denote the lattice parameters, which are identical in the cubic $Fm\bar{3}m$ structure. The symbols, h, k and l represent the Miller indices of the diffracting planes and can be obtained from reported $AgSbTe_2$ diffraction data in the literature.

Equation 3:

**Microstructural Characterization**

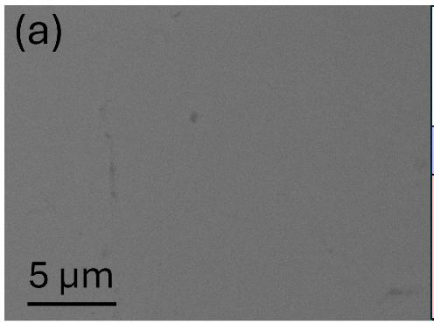


(b)

$Ag_{0.88}Sb_{1.03}Te_2$

| Region | Atomic % |
|---|---|
| Ag (%) | 22.5 |
| Sb (%) | 26.3 |
| Te (%) | 51.2 |

Figure S1 Microstructural observation of $AgSbTe_2$. (a) SEM image, (b) Quantitative compositional analysis through EDS.

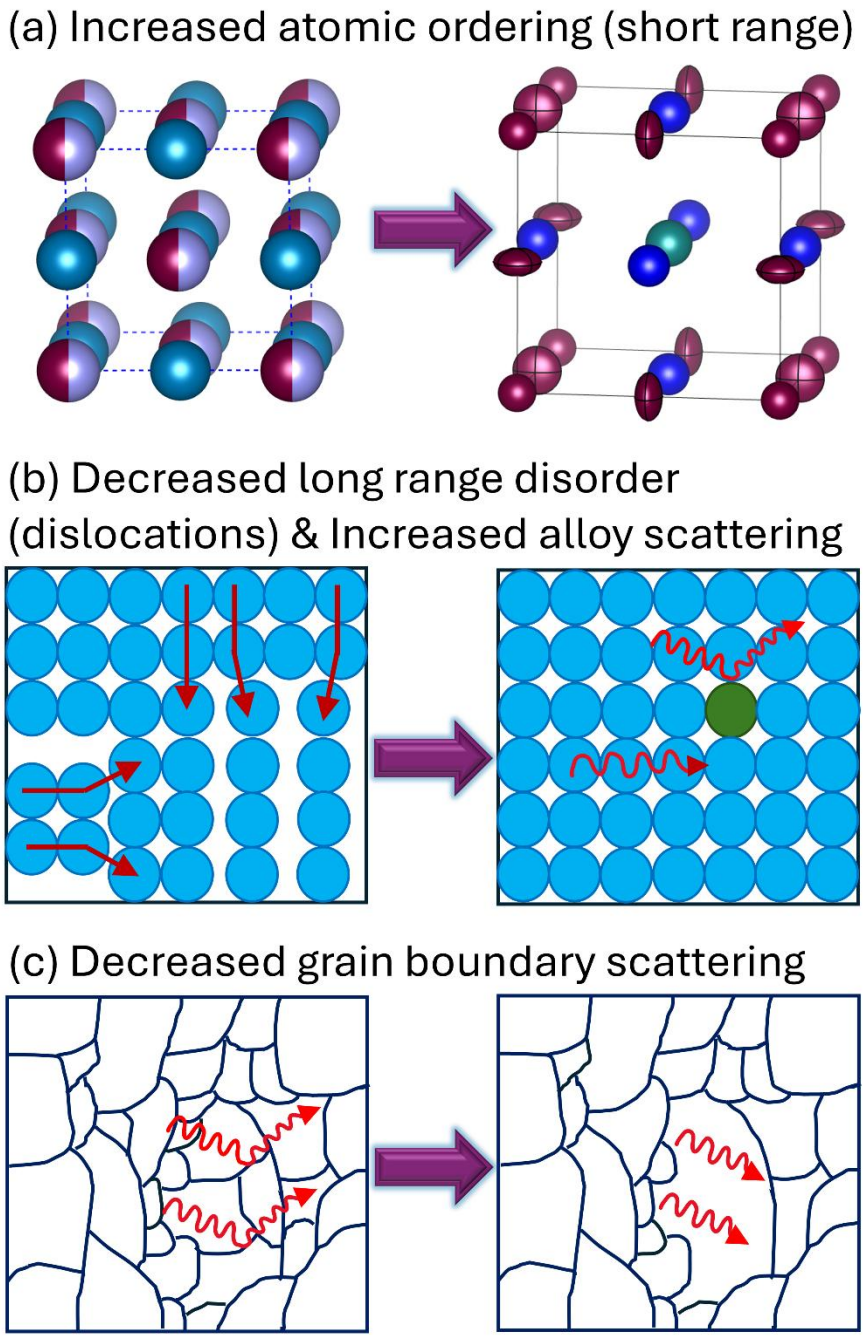


Figure S2 Schematic showing the impact of Ge doping on short and long-range disorder. (a) increased atomic ordering, (b) decreased density of dislocations and increased alloy scattering, (c) increased grain size decreasing grain boundary scattering.

Table S1 Structural parameters obtained from the PDF refinement of $AgSb_{0.94}Ge_{0.06}Te_2$

| element | x | y | z | $U^{11}$ | $U^{22}$ | $U^{33}$ |
|---|---|---|---|---|---|---|
| Te1 | 0.0 | 0.5 | 0.0 | 0.0270 | 0.0085 | 0.0270 |
| Te2 | 0.0 | 0.0 | 0.0 | 0.0170 | 0.0170 | 0.0170 |
| Sb1 | 0.5 | 0.5 | 0.5 | 0.0254 | 0.0254 | 0.0254 |
| Ag | 0.5 | 0.5 | 0.5 | 0.0205 | 0.0205 | 0.0205 |
| Sb2 | 0.5 | 0.5 | 0.0 | 0.0006 | 0.0006 | 0.0006 |

| Composition | η (%) | Power Density ($mWcm^{-2}$) | ΔT (K) | Ref | Setup |
|---|---|---|---|---|---|
| $AgSb_{0.94}Ge_{0.06}Te_2$ | 4.3 | 276 | 370 | This work | 1-leg |
| 4 mol% Y doped $AgSbTe_2$ | - | 388 | 334 | [1] | 4-leg |
| $Ag_{1.02}Ge_{0.02}Sb_{0.96}Te_2$ | 7 | 282 | 350 | [2] | 1-leg |
| $Ag_{0.98}SbTe_2$ | - | 268 | 325 | [3] | 2-leg |
| $AgSbTe_2$ | 13.3 | - | 370 | [4] | 1-leg |
| $(AgSbTe_2)_{0.98}$ | 11.2 | - | 323 | [5] | 1-leg |
| $(AgAlSe_2)_{0.02}$ | 5.2 | - | 323 | | 2-leg |
| $AgSb_{0.97}Fe_{0.03}Te_{2.01}$ | 10 | - | 323 | [6] | 4-leg |
| $AgSb_{0.96}Hg_{0.04}Te_2$ | 8.4 | 450 | 325 | [7] | 4-leg |
| $AgSb_{0.94}Sn_{0.06}Te_2$/ $Yb_{0.25}Co_{3.75}Fe_{0.25}Sb_{12}$ | 12.1 | 1130 | 370 | [8] | Uni-couple |
| $AgSbTe_2$ | 7.3 | - | 290 | [9] | 1-leg |

**References**


1. Taneja, V.; Das, S.; Dolui, K.; Ghosh, T.; Bhui, A.; Bhat, U.; Kedia, D. K.; Pal, K.; Datta, R.; Biswas, K., High Thermoelectric Performance in Phonon-Glass Electron-Crystal Like $AgSbTe_2$. *Advanced Materials* **2024,** *36* (6), 2307058.

2. Chen, B. C.; Wang, K. K.; Wu, H. J., Cation modulation in $AgSbTe_2$ realizes carrier optimization, defect engineering, and a 7% single-leg thermoelectric efficiency. *Small* **2024,** *20* (36), 2401723.

3. Pathak, R.; Xie, L.; Das, S.; Ghosh, T.; Bhui, A.; Dolui, K.; Sanyal, D.; He, J.; Biswas, K., Vacancy controlled nanoscale cation ordering leads to high thermoelectric performance. *Energy & Environmental Science* **2023,** *16* (7), 3110-3118.

4. Zhang, Y.; Li, Z.; Singh, S.; Nozariasbmarz, A.; Li, W.; Genç, A.; Xia, Y.; Zheng, L.; Lee, S. H.; Karan, S. K., Defect-engineering-stabilized $AgSbTe_2$ with high thermoelectric performance. *Advanced Materials* **2023,** *35* (11), 2208994.

5. Zhang, K.; Liu, S.; Wang, X.; Wu, S.; Xiong, Q.; Wang, X.; Chen, J.; Wang, G.; Zhang, B.; Fu, H., Dual alloying enables high thermoelectric performance in $AgSbTe_2$ by manipulating carrier transport behavior. *Advanced Functional Materials* **2024,** *34* (34), 2400679.
6. Zhang, K.; Wang, J.; Liu, S.; Ji, X.; Gao, C.; Zhang, B.; Wang, G.; Wang, G.; Wang, Y.; Zhou, Y., Enhanced thermoelectric performance in $AgSbTe_2$ with extremely low thermal conductivity via grain boundary defects. *Applied Physics Letters* **2025,** *126* (8), 083902.
7. Bhui, A.; Das, S.; Arora, R.; Bhat, U.; Dutta, P.; Ghosh, T.; Pathak, R.; Datta, R.; Waghmare, U. V.; Biswas, K., Hg doping induced reduction in structural disorder enhances the thermoelectric performance in $AgSbTe_2$. *Journal of the American Chemical Society* **2023,** *145* (46), 25392-25400.
8. Zhang, Y.; Xing, C.; Wang, D.; Genç, A.; Lee, S. H.; Chang, C.; Li, Z.; Zheng, L.; Lim, K. H.; Zhu, H., Realizing high power factor and thermoelectric performance in band engineered $AgSbTe_2$. *Nature communications* **2025,** *16* (1), 22.
9. Gong, Z.; Saglik, K.; Wu, J.; Suwardi, A.; Cao, J., Suppressing $Ag_2Te$ nanoprecipitates for enhancing thermoelectric efficiency of $AgSbTe_2$. *Nanoscale* **2023,** *15* (45), 18283-18290.